General DG30, apart from absorption correction on a Burroughs B6700. Scattering factors in the analytical form and anomalous dispersion factors were taken from ref 38. Final atomic coordinates are given in Table X and bond lengths and angles in Tables XI and XII of the supplementary material.

Crystal Structure Parameters for [Ni{Me_2(piperazine)$_2$3,6-durene-[16]cyclidene}](PF_6)$_2$: $C_{38}H_{58}N_8P_2F_{12}Ni$ (plus solvent); monoclinic; space group $P2_1/c$; at −80 °C, a = 9.738 (2) Å, b = 23.710 (6) Å, c = 21.380 (9) Å, β = 94.72 (3)°, U = 4920 (3); at −100 °C, a = 9.772 (2) Å, b = 23.733 (6) Å, c = 21.278 (6) Å, β = 94.97 (2)°, U = 4916 (3) Å, M = 975.5; Z = 4; D_c = 1.32 g cm^{-3}; Mo Kα radiation; T = −80 °C; λ = 0.71069 Å; crystal character, well-formed laths; crystals from acetonitrile. Data collection attempted with a Syntex $P2_1$ four-circle diffractometer. Despite holding crystals at −80 and −100 °C with the Syntex LT-1 attachment, the crystals decomposed rapidly (>50% after 30 h). The best attempt gave 800 reflections and less than a complete 0–35° (2θ) shell. Attempts to solve the structure from these data were not successful, and the problem was abandoned.

Acknowledgment. The financial support of the US National Institutes of Health, Grant GM10040, and of the US National Science Foundation, Grant CHE-8402153, is greatly appreciated. FT-NMR spectra at 11.75 T (500 MHz) and 7.0 T (300 MHz) were obtained at The Ohio State University Chemical Instrument Center using equipment funded in part by NIH Grand 1 S10 RR01458-01A1. The guidance of Dr. C. E. Cottrell was especially helpful. The collaboration between The Ohio State University and The University of Warwick was greatly aided by a NATO travel grant.

Supplementary Material Available: Relaxation data, atomic coordinated, isotropic thermal parameters, bond lengths and bond angles (8 pages). Ordering information is given on any current masthead page.

Novel Pathways for Ligand Substitution Reactions of Dinuclear Platinum(I) Complexes

Reed J. Blau[†] and James H. Espenson*

Contribution from the Ames Laboratory and Department of Chemistry, Iowa State University, Ames, Iowa 50011. *Received April 19, 1985*

Abstract: The terminal halide and/or triphenylphosphine ligands L in dinuclear platinum(I) complexes $[Pt_2L_2(\mu\text{-dppm})_2]^{n+}$ (where dppm = $Ph_2PCH_2PPh_2$) undergo ready substitutions. The reaction of $[Pt_2Cl_2(\mu\text{-dppm})_2]$, abbreviated (Cl--Cl), with PPh_3 follows a second-order rate law, with k = 15.2 ± 0.7 M^{-1} s^{-1} at 25 °C in CH_2Cl_2. The product is exclusively $(Cl\text{--}PPh_3)^+$; $(Ph_3P\text{--}PPh_3)^{2+}$ forms only in a more polar solvent like methanol. The complex $(Ph_3P\text{--}PPh_3)^{2+}$ reacts in CH_2Cl_2 with halide ions (X^- = Cl^-, Br^-, and I^-) also to yield $(X\text{--}PPh_3)^+$. In the presence of inert salts such as perchlorates, the reaction proceeds by rate-limiting dissociation of PPh_3, unusual for square-planar, 16-electron platinum, but further evidence for the large trans influence of the metal–metal bond. In the absence of such salts, however, the reaction occurs in three distinct kinetic stages, although eventually leading to $(Cl\text{--}PPh_3)^+$. One of the intermediates can be stabilized at low temperature; its ^{31}P NMR spectrum identifies it (for X^- = I^- and Cl^-) as a species containing both bridging and chelating dppm, $[Pt_2(X)(PPh_3)(\mu\text{-dppm})(\eta^2\text{-dppm})]^+$. Substitution of PPh_3 in $(Ph_3\text{--}PPh_3)^{2+}$, like the "A"-frame forming reactions of the same complex, starts with dissociation of one arm of a bridging dppm ligand.

Compounds containing two or more metal atoms have attracted much recent interest,[1] in part because of the analogies drawn between homogeneous and heterogeneous catalysis. The insertion of atoms and small molecules into metal–metal bonds leads to "A"-frame structures. Thus platinum(I) complexes containing bridging bis(diphenylphosphino)methane ligands, $[Pt_2Cl_2(\mu\text{-dppm})_2]$ and $[Pt_2(PPh_3)_2(\mu\text{-dppm})_2]^{2+}(PF_6^-)_2$ abbreviated[2] as (Cl--Cl) and $(Ph_3P\text{--}PPh_3)^{2+}$, react in dichloromethane with diazomethane, carbon monoxide, sulfur, sulfur dioxide, and hydrogen chloride.[3] They yield so-called molecular "A"-frame complexes $Pt_2Cl_2(\mu\text{-Y})(\mu\text{-dppm})_2$ and $[Pt_2(PPh_3)_2(\mu\text{-Y})(\mu\text{-dppm})_2]^{2+}$, respectively, with Y = CH_2, CO, S, SO_2, and H^+; e.g., eq 1, L = Cl^-, PPh_3; and R = CH_2N_2, CO, S_8, SO_2, HCl.

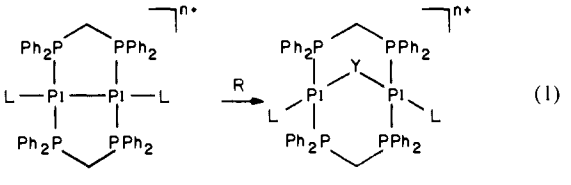

(1)

Although kinetics and other data suggest a direct bimolecular reaction for (Cl--Cl), data for the complex $(Ph_3P\text{--}PPh_3)^{2+}$ suggest[5] an intermediate derived by dissociation of one arm of the bridging diphosphine ligand.

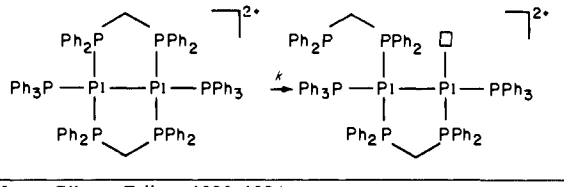

(2)

[†] Henry Gilman Fellow, 1983–1984.

We sought to substantiate the involvement of the "chelate-opened" intermediate by other evidence. If the $(Ph_3P\text{--}PPh_3)^{2+}$ is, indeed, too hindered to allow direct attack (by virtue of the seven phenyl groups around each platinum atom), then its other reactions, including ligand substitution, would be subject to the same effect.[6-8]

Thus we considered reactions leading to the mixed halide–phosphine complexes, $[Pt_2(X)(PPh_3)(\mu\text{-dppm})_2^+]$ or $(X\text{--}PPh_3)^+$. They can be formed not only by halide addition to $(Ph_3P\text{--}PPh_3)^{2+}$ but also by PPh_3 addition to (Cl--Cl). Each route to $(X\text{--}PPh_3)^+$ may adopt a different mechanism. This work concerns these issues as they relate to the formation of $(X\text{--}PPh_3)^+$ for X = Cl^-, Br^-, and I^-.

(1) Puddephatt, R. J. *Chem. Soc. Rev.* **1983**, *12*, 99.

(2) It is convenient for certain equations to abbreviate the structure of the parent complexes, which we have chosen to do by showing only the pair of terminal ligands bound to the $Pt_2(\mu\text{-dppm})_2$ core, as in the examples (Cl--Cl), $(Cl\text{--}PPh_3)^+$, and $(Ph_3P\text{--}PPh_3)^{2+}$.

(3) Brown, M. P.; Fisher, J. R.; Puddephatt, R. J.; Seddon, K. R. *Inorg. Chem.* **1979**, *18*, 2808.

(4) Muralidharan, S.; Espenson, J. H. *Inorg. Chem.* **1983**, *22*, 2786.

(5) Muralidharan, S.; Espenson, J. H. *J. Am. Chem. Soc.* **1984**, *106*, 8104.

(6) That is not to say that terminal ligand substitution, usually a facile process[7-9] for this family of Pt_2 complexes, constitutes a general or preferred route for insertion. In fact, we rather doubt that and consider that terminal substitution may more likely be a "dead-end" for A-frame formation. Quite irrespective of that, however, if insertion into the parent complex is indeed hindered, then other reactions, including substitution, may be as well.

(7) (a) Brown, M. P.; Franklin, S. J.; Puddephatt, R. J.; Thomson, M. A.; Seddon, K. R. *J. Organomet. Chem.* **1979**, *178*, 281. (b) Brown, M. P.; Puddephatt, R. J.; Rashidi, M.; Seddon, K. R. *J. Chem. Soc., Dalton Trans.* **1978**, 1540.

(8) Shimura, M.; Espenson, J. H. *Inorg. Chem.* **1984**, *23*, 4069.

0002-7863/86/1508-1962$01.50/0

Results and Interpretations

Initial Observations. The complex $(Cl--PPh_3)^+$ ultimately is formed from both sets of reactants, (a) (Cl--Cl) and PPh_3 and (b) $[(Ph_3P--PPh_3)^{2+}](PF_6^-)_2$ and Cl^-. The product has been fully characterized spectroscopically (^1H and $^{31}P\{^1H\}$ NMR, UV–vis) and structurally (single-crystal X-ray diffraction of its PF_6^- salt).[9]

Both reactions are equilibrium processes, as expected for ligand substitution. Although $(Cl--PPh_3)^+$ forms (eventually) under the various conditions used here, the species distribution can be altered by the expected concentration variables, $[PPh_3]$ and $[Cl^-]$, by the solvent and by the presence of the presumably "innocent" salts $R_4N^+ClO_4^-$ and $R_4N^+PF_6^-$. Not surprisingly, more polar solvents favor the dipositive bis(triphenylphosphine) complex; indeed, $[(Ph_3P--PPh_3)](PF_6)_2$(s) is prepared from (Cl--Cl) and PPh_3 in methanol.

Even in dichloromethane (used for both substitution and insertion reactions), striking differences were noted. Reaction between (Cl--Cl) and PPh_3 in dichloromethane yields $(Cl--PPh_3)^+$ readily and directly. In contrast, the opposite combination, $(Ph_3P--PPh_3)^{2+}$ and Cl^- yields *some* $(Cl--PPh_3)^+$ relative quickly, which implies a presumably straightforward route directly to product. In parallel (and in competition) with it, a substantial amount of the reaction proceeds by way of long-lived intermediates which are readily evident spectroscopically (^1H, ^{31}P, NMR; UV–vis). Only after several hours are the reactants converted entirely to $(Cl--PPh_3)^+$.

To complicate the picture further, the reactions are very sensitive to added electrolytes. The variation of $[Cl^-]$, added usually as $Et_4N^+Cl^-$, leads to the expected equilibrium shifts. In addition, however, this salt and even the salts of presumably "innocent" anions, e.g., R_4N^+ ClO_4^- and R_4N^+ PF_6^-, alter the rates of various reaction steps and the proportions and lifetimes of different intermediates. These effects reflect the extensive association of the cationic dinuclear complexes with various anions. This sensitivity extends even to the experimentally simpler reactions of (Cl--Cl) with PPh_3. The ^1H NMR spectrum of (Cl--Cl) is perceptibly shifted (but not altered in form) by $R_4N^+An^-$. Association defines the ion-paired species present and alters their reactivity.

Reaction of (Cl--Cl) with PPh_3. The reactants along with $(Cl--PPh_3)^+$ were detected by ^{31}P NMR from a 1:1 reaction at 33 mM; some of the dichloro complex remained even with a 3:1 stoichiometric excess of PPh_3. The extent of binding of PPh_3 was determined by integration of the ^{31}P NMR spectrum. If the equilibrium is written to incorporate ion-association of the product explicitly,

$$(Cl--Cl) + PPh_3 = [(Cl--PPh_3)^+]^*Cl^- \qquad (3)$$

the equilibrium constant is $K_3 = (5.7 \pm 0.8) \times 10^3$ M^{-1} (in CD_2Cl_2 at ambient temperature).[10]

A large excess of Cl^- added to a solution of independently-prepared $[(Cl--PPh_3)^+](PF_6^-)$ partially reverses the reaction since $[PPh_3]$ is low. Addition of Cl^- to solutions having excess PPh_3, on the other hand, has relatively little effect since PPh_3 is bound more strongly than Cl^-.[10] The binding of other ligands relative L to Cl^- increases in the order L = $AsPh_3$ < P(*o*-tol)$_3$ < PPh_3 < η^1-dppm.

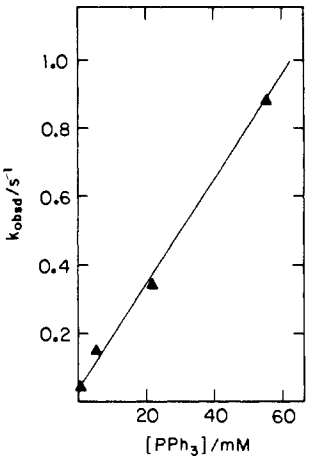

Figure 1. The pseudo-first-order rate constant for reaction of $Pt_2Cl_2(\mu$-dppm$)_2$ with PPh_3 varies linearly with $[PPh_3]$ in solutions containing added $Et_4N^+Cl^-$ (0.5 mM). The second-order rate constant is 15.2 ± 0.7 M^{-1} s^{-1} at 25.0 °C in CH_2Cl_2.

The rate of reaction was determined spectrophotometrically at low $[(Cl--Cl)]_0$, 0.1 mM, and varying $[PPh_3]$, in the presence of added 0.5 mM $Et_4N^+Cl^-$. Under these conditions the reaction followed pseudo-first-order kinetics. The plot of k_{obsd} vs. $[PPh_3]$ is linear, as shown in Figure 1, with a slope (k_L) of 15.2 ± 0.7 M^{-1} s^{-1} at 25 °C in CH_2Cl_2. There is also a small and relatively uncertain intercept, 0.04 ± 0.02 s^{-1}. (The latter is *not* due to the reaction being reversible under these conditions but probably represents a minor pathway.[11]) The major pathway presumably proceeds by associative substitution at the platinum center, like ordinary reactions at square-planar, 16-electron platinum centers. As previously noted,[8] the rate is strongly enhanced (as compared to ordinary Pt substitution reactions) by the presence of the Pt–Pt bond trans to the leaving halide ion.

The importance of ion-association in this system is emphasized by results for the same reaction in the initial absence of Cl^-. The rate is then *much* higher, and first-order kinetics are not well obeyed (see Figure 2). The initial rate is about 10^2 higher, with $k_L = 1.9 \times 10^3$ M^{-1} s^{-1}. As the reaction progresses, the rate becomes lower, and a first-order fit less satisfactory. This is because the Cl^- being released associates with the reactant to produce a less reactive ion-paired form of the parent complex.

Addition of 0.020 M $(n\text{-}Bu)_4N^+ClO_4^-$ to an equilibrium mixture of (Cl--Cl) and $(Cl--PPh_3)^+$ causes a significant shift in the equilibrium of eq 3 to the right. We attribute this to the increased stabilization of $(Cl--PPh_3)^+$ by association[10] with ClO_4^- as well as Cl^-.

Reactions of Halide with $[(Ph_3P--PPh_3)^{2+}](PF_6^-)_2$. These reactions are extraordinarily sensitive to electrolytes. For example, consider the reaction of $(Ph_3P--PPh_3)^{2+}$ (2.0×10^{-5} M) with $(n\text{-}Bu)_4N^+I^-$ (2.0×10^{-4} M) in dichloromethane at 10 °C. With the "innocent" salt $(n\text{-}Bu)_4N^+$ ClO_4^- (0.020 M) added, the substitution product $(I--PPh_3)^+$ is formed in nearly quantitative yield; this occurs directly (see Figure 3a) in a single stage reaction that follows first-order kinetics, as detailed subsequently.

Without that salt, on the other hand, the reaction begins much more rapidly but ultimately requires many hours and three distinct stages for completion. The accompanying spectrophotometric changes are illustrated in Figures 3b and 4. The first stage, complete within ~1 min, is characterized by absorbance increases at >410 nm and decreases at <410 nm. This reaction, as justified subsequently, is dissociation of one arm of the dppm bridge; it

(9) Blau, R. J.; Espenson, J. H.; Kim, S.; Jacobson, R. A. *Inorg. Chem.* **1986**, *25*, 757.

(10) The representation given in eq 3 is, to some extent, arbitrary, since appreciable concentrations of free $(Cl--PPh_3)^+$ coexist with the ion pair. This is especially prevalent in solutions to which additional Cl^- or other anions are not added. This was confirmed spectrophotometrically in a series of measurements in 1,2-dichloroethane. The strong absorbance increases accompanying coordination of triphenylphosphine are functions not only of $[PPh_3]$ but also of the concentration of added chloride ions or other anions. The determinations were only semiquantitative, however, and precise equilibrium constants cannot be quoted. Roughly speaking, the phenomenon referred to occurs at anion concentrations consistent with ion-pair formation constants of the expected magnitude. Considering literature values for association of ions of charges 1^+ and 1^- in dichloromethane and 1,2-dichloroethane of the order of 10^3–10^5 M^{-1} [Algra, G. P.; Balt, S. *Inorg. Chem.* **1982**, *20*, 1102. Ito, K. *Inorg. Chem.* **1983**, *22*, 2872], the species in eq 3 predominate at high $[(Cl--L)^{n+}]_{tot}$, e.g., 33 mM. However, at much lower Pt_{tot} concentrations e.g., 0.1 mM, appreciable concentrations of free $(Cl--PPh_3)^+$ coexist with the ion pair. This is especially true in the absence of added Cl^- or other anions. Experimental evidence suggests that the uncharged molecule (Cl--Cl) also interacts with chloride ions. Thus eq 3 is not always representative of the species in solution.

(11) The absorbance changes are essentially the same in each of the kinetics experiments. This confirms that the reaction goes to completion. More likely, the small intercept either reflects a minor, $[PPh_3]$-independent pathway or is another manifestation of ion-association effects; in any event, it is not a principal feature of the mechanism.

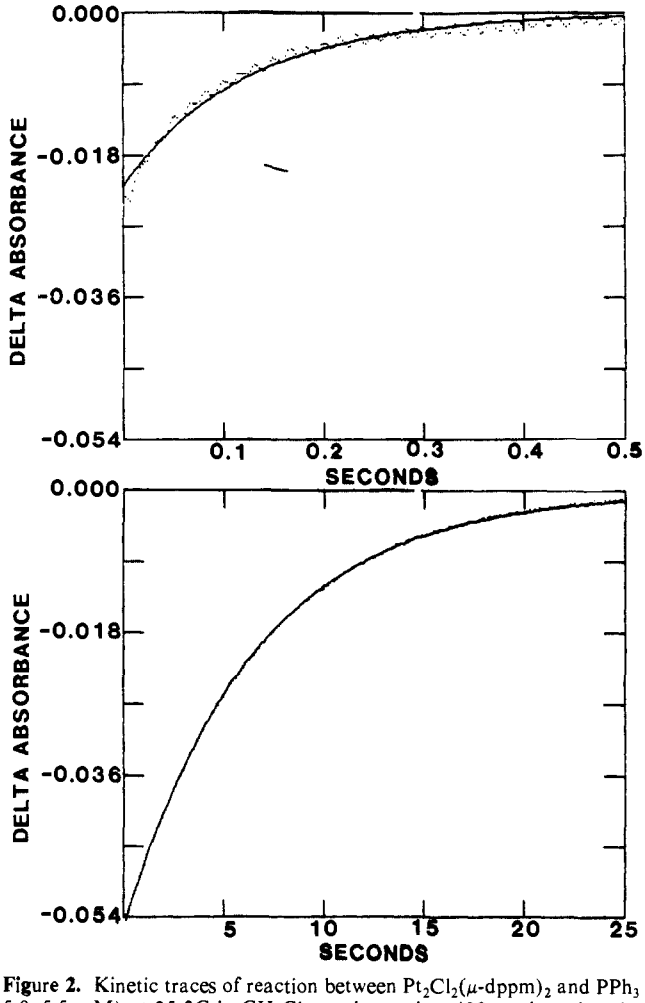

Figure 2. Kinetic traces of reaction between $Pt_2Cl_2(\mu\text{-dppm})_2$ and PPh_3 5.0–5.5 mM) at 25 °C in CH_2Cl_2 as observed at 400 nm by using the stopped-flow method. Runs are shown in the absence of added Cl^- (top curve, $k \sim 8\ s^{-1}$) and with 0.5 mM $Et_4N^+Cl^-$ added (lower curve, $k = 0.15\ s^{-1}$). Not only is the former faster but the data points (dots) do not fit well to first-order kinetics (calculated line, see text).

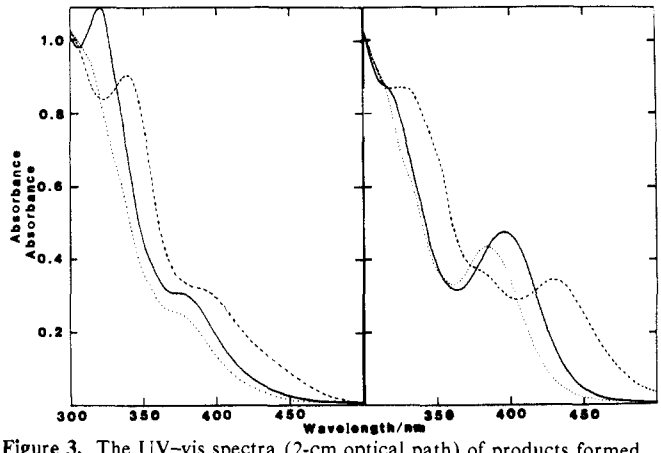

Figure 3. The UV–vis spectra (2-cm optical path) of products formed from $[Pt_2(PPh_3)_2(\mu\text{-dppm})_2^{2+}](PF_6^-)_2$ (0.02 mM) and $R_4N^+X^-$ (0.2 mM) in CH_2Cl_2 at 10 °C. With added 20 mM $(n\text{-Bu})_4N^+ClO_4^-$ (a, left), the 1:1 complexes $[Pt_2X(PPh_3)(\mu\text{-dppm})_2]^+$ are formed without the intervention of intermediates. Without added perchlorate (b, right), distinctly different species are formed; the latter spectra were recorded at roughly the time of complete formation of the intermediate identified as containing chelated dppm. The dotted, solid, and dashed lines refer to Cl^-, Br^-, and I^-, respectively.

is termed the "*chelate-opening*" reaction. The second stage, occurring (for iodide) over the next 30 min, leads to absorbance decreases at >385 nm and increases at <385 nm. This is primarily the formation of a complex containing chelated η^2-dppm, identified

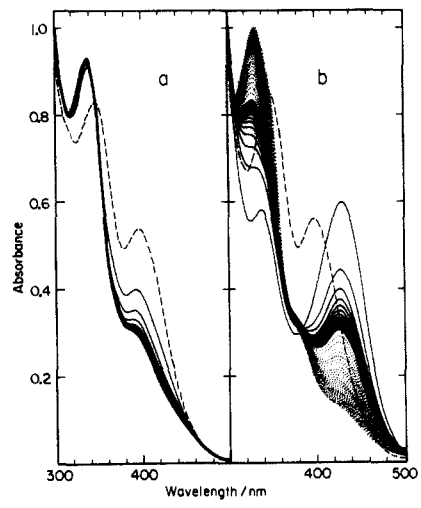

Figure 4. Timed tracings of the UV–vis spectral changes accompanying the same reactions as in Figure 4 for X = I^-. The reaction with ClO_4^- added (left) proceeds smoothly to the 1:1 complex, whereas that without (right) occurs in three stages. The first stage, already complete on mixing (dashed line), leads to the formation of new peaks (at 339 and 426 nm); in scans (solid lines) shown at 2.0 min intervals, the former intensifies and shifts (to 322 nm), and the latter bleaches. Finally, shown in 10-min scans over 2 h (dotted lines), the shoulders (435 and 390 nm) and peak (at 332 nm) of the 1:1 complex develop.

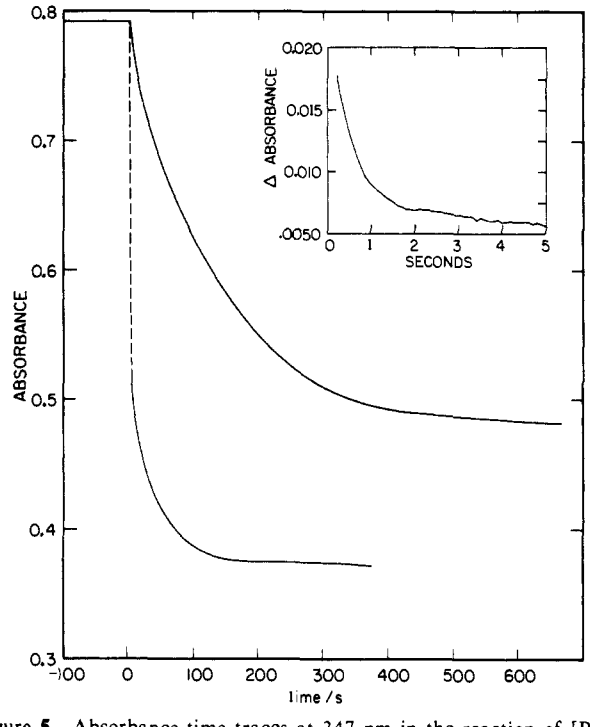

Figure 5. Absorbance-time traces at 347 nm in the reaction of $[Pt_2(PPh_3)_2(\mu\text{-dppm})_2^{2+}]$ with Br^- in CH_2Cl_2. In the presence of 0.020 M $(n\text{-Bu})_4N^+ClO_4^-$ (upper curve), the absorbance changes smoothly as the 1:1 complex is formed. In its absence (lower curve), a faster reaction forming the η^2-dppm (chelated) intermediate occurs; preceding it there is an initial very rapid changed measurable by the stopped-flow method (inset, at 370 nm), which is the formation of the ring-opened intermediate.

by ^{31}P NMR. (Especially for the chloride reaction, the second stage is accompanied by partial occurrence of the "direct" pathway involving PPh_3 dissociation.) The third and final stage, requiring several hours, yields $(I\text{-}\text{-}PPh_3)^+$ essentially quantitatively, just as happened within a few minutes when the perchlorate salt was present. The final products from both have the same ^{31}P spectrum and are identical with $(I\text{-}\text{-}PPh_3)^+$ from the reaction of (I--I) with PPh_3. Similar effects were found for Cl^- and Br^-, on comparable but not identical time scales, although the spectrophotometric

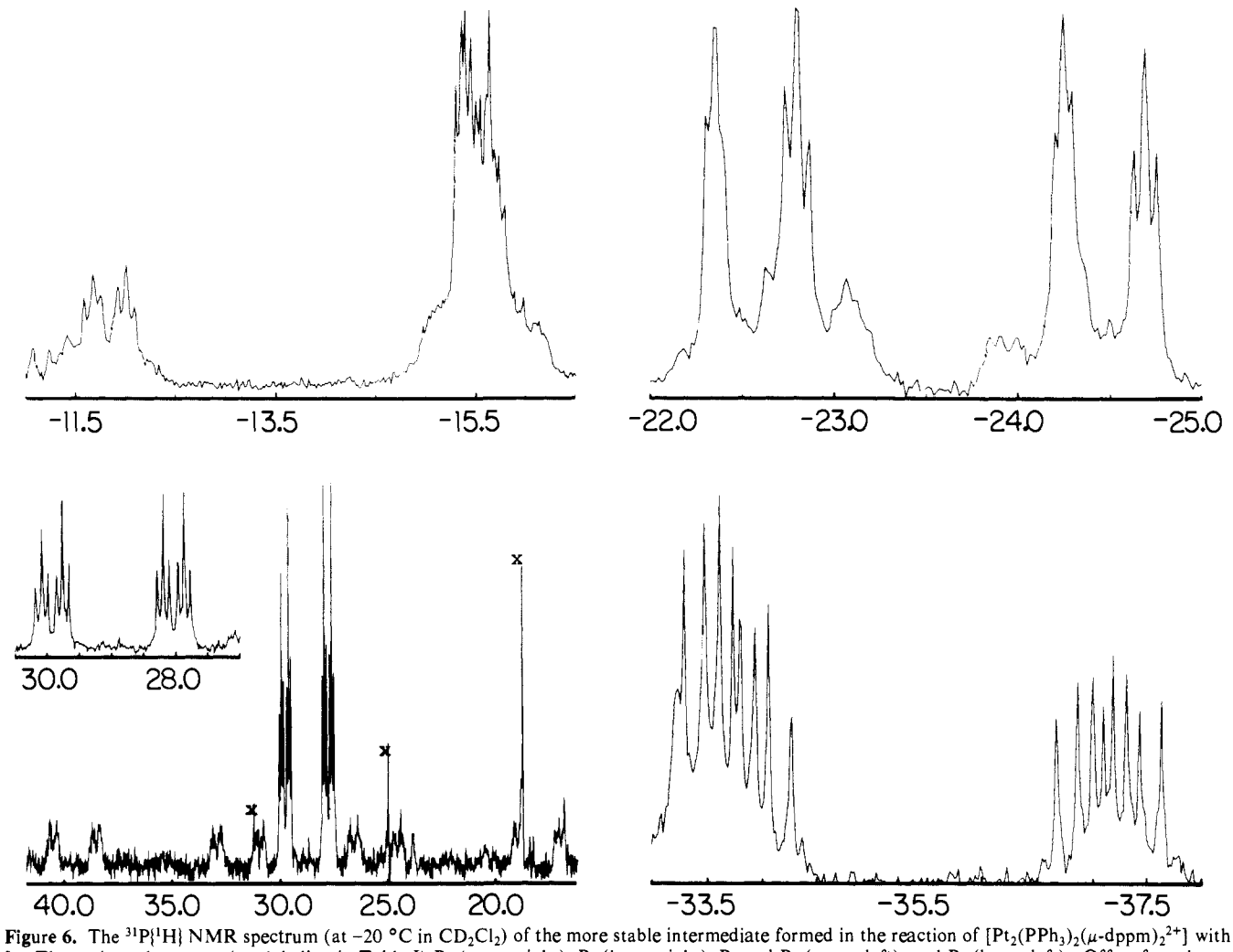

Figure 6. The $^{31}P\{^1H\}$ NMR spectrum (at −20 °C in CD_2Cl_2) of the more stable intermediate formed in the reaction of $[Pt_2(PPh_3)_2(\mu\text{-dppm})_2^{2+}]$ with I^-. The regions shown are (see labeling in Table I) P_1 (upper right), P_2 (lower right), P_3 and P_4 (upper left), and P_5 (lower left). Offset from latter is an expanded portion of the central resonance. Peaks marked "X" are due to the "folding over" of the PF_6^- resonance at ca. −150 ppm.

changes are not as dramatic. Absorbance-time profiles at a single wavelength during the Br^- reaction are shown in Figure 5.

The sequence being described is represented in eq 4 with 4a representing the direct path and 4b the sequence of intermediates

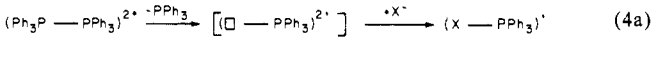

(4a)

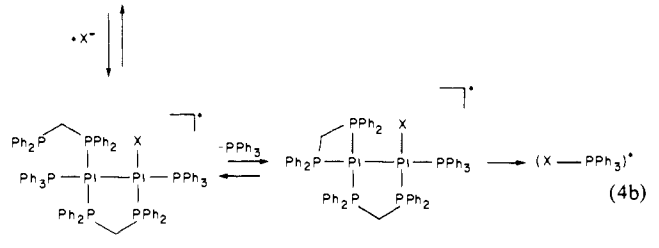

(4b)

that tends to dominate when strong electrolytes are absent. The symbol □ represents a coordination site, normally filled, which is vacant in an intermediate.

None of the highly-absorbing intermediates formed from $(Ph_3P\text{--}PPPh_3)^{2+} + X^-$ in the absence of perchlorate is the product $(X\text{--}PPh_3)^+$, formed from the opposite combination, $(X\text{--}X) + PPh_3$. To complicate the issue further, the prominence of the intermediates is a function of concentration. When run at higher reagent concentrations to obtain better NMR spectra, the former reaction yields more $(Cl\text{--}PPh_3)^+$ directly. In effect, the higher reagent concentrations correspond to a higher electrolyte concentration, thus favoring the direct path of eq 4a over 4b.

Characterization of the η^2-dppm Chelated Intermediate. The iodide reaction gives the best yield of this intermediate and is thus the most favorable case for NMR examination. Portions of its $^{31}P\{^1H\}$ spectrum (omitting regions obscured by resonances from the portion of directly-formed product) are shown in Figure 6. It is stable for many hours at −20 °C but decomposes to $(I\text{--}PPh_3)^+$ within 90 min at room temperature. Since the NMR spectrum disappears in concert with the 384-nm absorption maximum, the two can be attributed to the same species.

The intermediate is believed to contain an η^2-dppm chelate on the basis of its ^{31}P spectrum (Table I) for the iodo and chloro complexes (the latter of lower quality). Because four types of dppm–phosphorus atoms are present, as compared to two in $(X\text{--}PPh_3)^+$, each appears as an even more complex[9] set of multiplets due to additional P–P coupling. The chelated intermediates are characterized by large P–P coupling constants. In contrast to $[Pt_2(\mu\text{-dppm})_2(PR_3)_2]^{2+}$ structures,[7a] which have no readily observable P–P coupling constants larger than 60 hz,[13] the intermediate shows values of trans-$^2J(P_2,P_4)$ and trans-$^3J(P_1,P_3)$ greater than 400 and 200 Hz, respectively. This happens because, in $[Pt_2(\mu\text{-dppm})_2(PR_3)_2]^{2+}$ complexes, the trans-dppm and trans-$R_3P\text{–}Pt\text{–}Pt\text{–}PR_3$ phosphorus atoms are symmetry-related, unlike those in the chelated intermediate which can have no symmetry higher than C_s.

Consistent with the proposed structure (the middle formula in eq 4b), similar effects are found within the pairs of bridging and chelating dppm phosphorus nuclei. The resonances at −13.5 and

(12) Conditions were not found in which the chelated intermediate predominated over the $(Cl\text{--}PPh_3)^+$ product at an NMR concentration; at most, ca. 25% yield was obtained at the concentrations needed for reliable spectra.

(13) The single exception to this appears to be the compound with $PR_3 = PMe_2Ph$, whose NMR spectrum is discussed in ref 7a.

Table I. $^{31}P\{^1H\}$ NMR Data for the Chelated Intermediate $[Pt_2X(PPh_3)(\mu\text{-dppm})(\eta^2\text{-dppm})]^+$ for X = I and Cl[a,b]

atom	chemical shifts (ppm)		coupling constants (Hz)						
			J_{PP}[c] with					J_{PtP}[d] with	
	X = I	X = Cl	P_1	P_2	P_3	P_4	P_5	Pt_A	Pt_R
P_1	−23.5	−22.7		53.4	5.7	5.7	228	380	1607
P_2	−35.5	−25.5	43.0		23.3	409	39.3		2706 (2796)
P_3	−15.6	−11.3	0	14.2		40.0	11.2	4305 (4215)	
P_4	−13.5	−5.5	9.3	405	46.0		11.2		3405 (3022)
P_5	28.8	31.8	239	39.1	8.5	8.5		2457 (2213)	723 (812)

[a] In CD_2Cl_2; the solution was cooled to −20 °C immediately after mixing at room temperature. [b] The labeling of phosphorus atoms is as shown, with Pt_A and Pt_R being the respective atoms bound and not bound to X

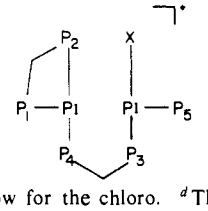

[c] The J_{PP}'s above the diagonal are for the iodo, those below for the chloro. [d] The J_{PtP}'s are for the iodo, with chloro values in parentheses.

−15.6 ppm are closer to those for complexes containing bridging dppm, such as $(Cl\text{-}\text{-}PPh_3)^+$ (+2 and −2 ppm)[9] and $(Ph_3P\text{-}\text{-}PPh_3)^{2+}$ (−5.5 ppm).[5] The others, at −23.5 and −35.5 ppm, resemble those in $PtCl(CH_3)(\eta^2\text{-dppm})$ and other Pt(II) complexes containing η^2-dppm (−36 to −40 ppm).[14] These η^2-dppm–phosphorus chemical shifts are similar to the chemical shift of free dppm (−23 ppm).

The magnitudes of the Pt–P coupling constants are in harmony with the suggested structure. The values of $^1J(Pt,P)$, for instance, vary according to the trans influence of group "L" in several P_n–Pt–L linkages:[15-24] L = Pt (P_1, 2706 Hz; P_5, 2457) < L = P (P_2, 2706; P_4, 3045) > L = I (P_3, 4305). The two-bond couplings between cis-disposed platinum and phosphorus atoms (P_2–Pt_A, P_4–Pt_A, and P_3–Pt_R) are sufficiently small so that the corresponding ^{195}Pt satellites are obscured by the complexity of the central multiplets. For the same reason, cis-$^2J(Pt,P)$ are often not observed unambiguously in complexes containing the $Pt_2(\mu\text{-dppm})_2$ core.[7a,16,24] On the other hand, the readily observed couplings, trans-$^2J(Pt_R,P_5)$ and trans-$^2J(Pt_AP_1)$, 723 and 380 Hz, respectively, provide evidence for significant Pt–Pt bonding in the chelated intermediate. The values $^1J(Pt_R,P_1)$ = 1607 Hz and $^2J(Pt_A,P_1)$ = 380 Hz are significantly smaller than the ranges typically found when η^1-PR_3 is bound trans to the Pt–Pt bond in $(R_3P\text{-}\text{-}PR_3^{2+})$ complexes, 2000–2200 and 650–1000 Hz, respectively.[7a,16,17] They are consistent, however, with the proposed structure in which the P_1–Pt_R bond, weakened by the trans influence of the Pt–Pt bond,[15] is the weakest link in a strained four-membered chelate ring.

The P–P coupling constants also support the proposed structure. Notable amont these are (a) the trans-$^2J(P_2,P_4)$ of 405 Hz which

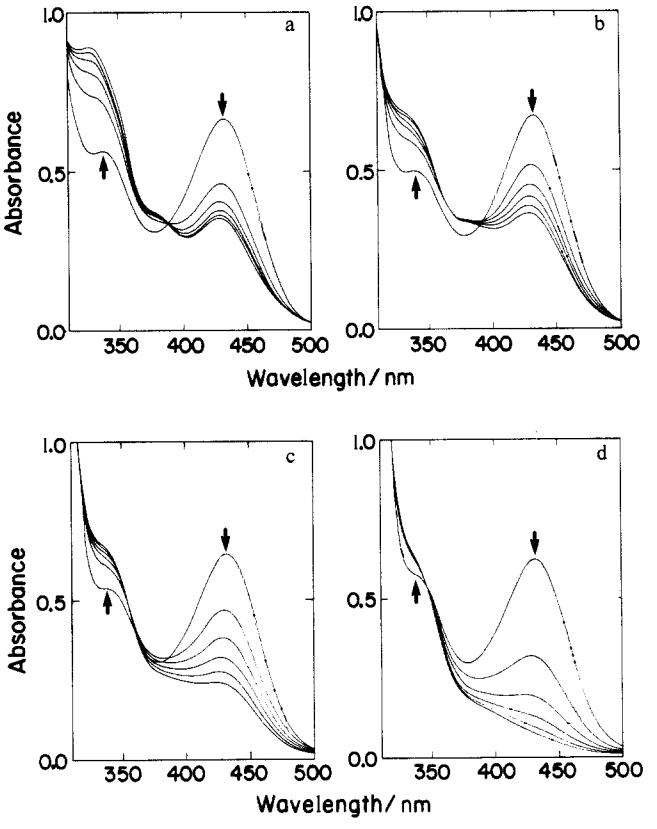

Figure 7. Scans of the UV-vis spectrum at 2.0-min intervals of a reaction (conducted in a spectrophotometer cell of 2-cm optical path at 10 °C in CH_2Cl_2) between 0.2 mM $[(n\text{-butyl})_4N]I$ and 0.02 mM $[Pt_2(\mu\text{-dppm})_2(PPh_3)_2]^{2+}$ with varying $[PPh_3]$ of (a) 0, (b) 0.2, (c) 0.8, and (d) 2.0 mM.

fits with those reported for Pt(II) complexes, 300–700 Hz and (b) $^3J(P,P)$'s: the value of $^3J(P_1,P_5)$, 228 Hz, which compares well with $(PhMe_2P\text{-}\text{-}PMe_2Ph)^{2+}$, 195 Hz, and values in the range of 160–180 Hz for $[(Ph_3P)_3(CO)Pt_2(\mu\text{-S})]$ and related compounds.[25] The values of $^3J(P_1,P_4)$ and $^3J(P_4,P_5)$, 5.7 and 11.2 Hz, are only half of $^3J(P_2,P_3)$ (23.3), which is not surprising from a Karplus correlation[26] since the dihedral angle in the former types is about 90° as compared to about 120° for the latter.

Precedents for chelated dppm are reasonably numerous[1] and include the mononuclear complex[25] $PtCl_2(\eta^2\text{-dppm})$. The most

(14) Cooper, S. J.; Brown, M. P.; Puddephatt, R. J. *Inorg. Chem.* **1981**, *20*, 1374.
(15) Blau, R. J.; Espenson, J. H. *Inorg. Chem.*, in press.
(16) Azam, K. A.; Brown, M. P.; Hill, R. J.; Puddephatt, R. J.; Yavari, A. *Organometallics* **1984**, *3*, 697.
(17) Brown, M. P.; Fisher, J. R.; Hill, R. H. Puddephatt, R. J.; Seddon, K. R. *Inorg. Chem.* **1981**, *20*, 3516.
(18) Pregosin, P. S.; Kunz, R. W. "NMR Basic Principles and Progress" Diehl, P., Fluck, E., Kosfeld, R., Eds.; Springer-Verlag: New York, 1979; Vol. 16.
(19) Manojlovic-Muir, Lj.; Muir, K. W.; Solomun, T. *Acta Crystallogr., Sect. B: Struct. Crystallogr. Cryst. Chem.* **1979**, *35*, 1237.
(20) Manojlovic-Muir, Lj.; Muir, K. W.; Solomun, T. *J. Organomet. Chem.* **1979**, *179*, 479.
(21) Mather, G. G.; Pidcock, A.; Rapsey, G. J. N. *J. Chem. Soc., Dalton Trans.* **1973**, 2095.
(22) Clark, H. C.; Dymarski, M. J.; Oliver, J. D. *J. Organomet. Chem.* **1978**, *154*.
(23) Fisher, J. R.; Mills, A. J.; Sumner, S.; Brown, M. P.; Thomson, M. A.; Puddephatt, R. J.; Frew, A. A.; Manojlovic-Muir, Lj.; Muir, K. W. *Organometallics* **1982**, *1*, 1421.
(24) Brown, M. P.; Puddephatt, R. J.; Rashidi, M.; Seddon, K. R. *J. Chem. Soc., Dalton Trans.* **1977**, 951.
(25) Hunt, C. T.; Matson, G. B.; Balch, A. L. *Inorg. Chem.* **1981**, *20*, 2270.
(26) Karplus, M. *J. Am. Chem. Soc.* **1963**, *85*, 2870.

immediate analogy to the intermediate in this reaction is the crystallographically-characterized compound[27] $[Pt_2(\mu\text{-dppm})(\eta^2\text{-dppm})_2]^{2+}$, which not only contains both types of dppm in the same complex but also has a Pt–Pt single bond.

Kinetics of the First Stage. The UV–vis spectra also illustrate the effects of added perchlorate ions; e.g., the reaction of 0.02 mM $(Ph_3P\text{--}PPh_3)^{2+}$ with 0.2 mM $Et_4N^+Br^-$ (Figure 5). The first stage of the reaction was followed by the stopped-flow method. In the absence of a perchlorate salt the reaction occurs partially by PPh_3 dissociation as well as chelate-opening.[28] The former is most prevalent for chloride, least for iodide. The reactions follow first-order kinetics; the rate constants at 10 °C in CH_2Cl_2 ar Cl^-, $k = 1.8 \pm 0.7\ s^{-1}$ (0.20–4.0 mM Cl^- concentration range); Br^-, 2.9 ± 0.1 (0.20–50.0 mM Br^-); and I^-, 0.25 ± 0.01 (1.0–10.0 mM I^-).

The rate constants are independent of the concentration of a given halide but do vary from one halide to another, being comparable for Cl^- and Br^- and nearly an order of magnitude smaller for I^-. The anion specificty is believed to reflect the extensive association of these halides under the reaction conditions; each ion pair reacts at a different rate. The steps in the mechanism at this point are as follows:

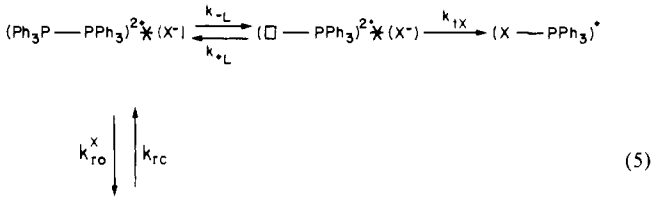

(5)

The expression for the pseudo-first-order rate constant derived from this mechanism is given in eq 6. It simplifies to eq 7 because

$$k_{obsd} = \frac{k_{-L}}{\{k_{+L}/k_{tX}\} + 1} + \frac{k^X_{ro}}{\{K_{cr}/k_{cX}\} + 1} \quad (6)$$

$$k_{obsd} = k_{-L} + k^X_{ro} \quad (7)$$

k proved to be independent of the concentraion of X^- but not its nature, and the relative proportions of PPh_3 dissociation and ring-opening are independent of $[PPh_3]$.

Similar experiments done with *two* halide ions present revealed a most unusual pattern of products and kinetics. For example, with both Cl^- and I^- (each at 1.2 mM), $(Ph_3P\text{--}PPh_3)^{2+}$ is converted almost entirely to the iodide-containing species, as demonstrated spectrophotometrically. The rate constant ($0.23 \pm 0.03\ s^{-1}$) was very close to the independently established value for I^- alone ($0.25 \pm 0.01\ s^{-1}$) but considerably lower than that for Cl^- alone ($1.9\ s^{-1}$). The unusual feature is that the product and the reaction rate in the mixture are those for I^-, not Cl^-. *It is as if the reaction, given a choice, followed the slower of two competing pathways.* Similarly, with Br^- and I^- together, the iodide product again is formed, and the rate constant ($0.43\ s^{-1}$) is much nearer the I^- value than the Br^-. We interpret these results to mean that each of the ion pairs reacts differently, and the strength of iodide ion pairing is the greatest. That ion pair is not only the predominant species but also the least reactive; association with halide ions lowers the chelate-opening rate constant. This provides additional proof for the important of ion pairs in controlling the reactivity. From the values given, the relative ion-pairing constants between $(Ph_3P\text{--}PPh_3)^{2+}$ and X^- can be estimated. They are in the ratio $24K_{Cl} < 8K_{Br} \sim K_I$.

Ion-pairing of ClO_4^- and PF_6^- is also extensive. This would lower the rate of ring opening, as demonstrated in the I^-/Cl^- comparison. This association appears to be the underlying reason why these otherwise innocent anions divert the reaction toward PPh_3 dissociation and away from halide ion trapping of the intermediate from the ring-opening reaction. The first-order rate constants in the presence of the innocent anions are much lower, and vary linearly with $[X^-]$, but extrapolate to an intercept which is independent of the nature of X^-. This pattern is consistent with the mechanism given once; the ion-pairing anion (but not the entering anion) in eq 5 is changed to perchlorate. The following expression then applies:

$$k_{obsd} = k_{-L} + (k^X_{ro}\, k'_{cX}/k_{rc})\cdot[X^-] \quad (8)$$

The X^--independent intercept of the plots suggested by eq 8 for $(Ph_3P\text{--}PPh_3)^{2+}\cdot(ClO_4^-)$ is $k_{-L} = (6.4 \pm 0.4) \times 10^{-3}\ s^{-1}$ at 10 °C in CH_2Cl_2 when ClO_4^- is added to provide a total salt concentration of 20 mM. The composite k's from the slopes of these plots are $1.22 \pm 0.06\ M^{-1}\ s^{-1}$ for Cl^- and $0.85 \pm 0.04\ M^{-1}\ s^{-1}$ for Br^-.

A further prediction made from this scheme is also borne out by the experimentally observed absorbance changes: with increasing $[X^-]$, an increasing proportion of the reaction should go by the ring-opening pathway. This also shows why the chelated intermediate derived from Cl^-, unlike that containing I^-, was formed in lower yields in the more concentrated solutions used for NMR measurements. Ion-pairing by the PF_6^- counter-ion is preferred over Cl^-, thus favoring direct formation of $(Cl\text{--}PPh_3)^+$. The ion pair formed by I^-, on the other hand, is tighter than that with PF_6^-. This favors the ring-opeing reaction and a higher yield of the η^2-dppm intermediate.

Addition of PPh_3 at low $[Cl^-]$ lowers the rate constant owing to the growing importance of the k_{+L} term in the mechanism of eq 5. The predicted form in this limit is

$$k_{obsd} = k_{-L}/\{1 + k_{+L}[PPh_3]/k_{tCl}[Cl^-]\} \quad (9)$$

A fit to this equation gives $k_{+L}/k_{tCl} = (4.0 \pm 0.2) \times 10^{-2}$ and $k_{-L} = (6.0 \pm 1.6) \times 10^{-3}\ s^{-1}$. The latter agrees with the more precise value of $6.4 \pm 0.4 \times 10^{-3}\ s^{-1}$ determined from the PPh_3-free experiments reported above.

Kinetics of Formation of the η^2-dppm Intermediate. This stage was monitored by conventional spectrophotometry, after completion of the first stage which occurred on the stopped-flow time scale. It was easily followed at 347 nm for Cl^- and Br^- and 400 nm for I^-, as shown in Figures 7 and 8. (As noted earlier, the timing of this transformation matches that of the ^{31}P signal for the chelated intermediate; this makes us confident that the spectrophotometric rates are being attributed correctly.) First-order kinetics were followed, and as anticipated from the nature of the chemical change, the rate constant (10 °C in CH_2Cl_2) is independent of $[X^-]$ (0.2–2.0 mM) but depends on the identity of X^-: $0.027 \pm 0.001\ s^{-1}$ (Cl^-), $0.029 \pm 0.004\ s^{-1}$ (Br^-), and $\sim 7 \times 10^{-4}\ s^{-1}$ (I^-).

The reaction scheme for this stage is as follows, with the measured rate constant attributed to $-k_{L'}$, representing loss of PPh_3 from the ring-open intermediate.

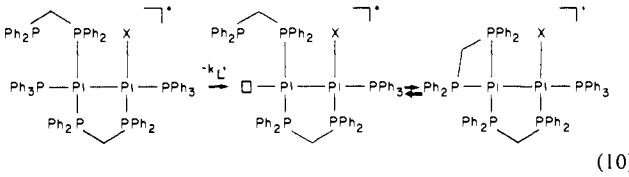

(10)

Further features of the scheme can also be discerned from these results. Without added PPh_3, the spectrum (Figure 7a) matched

(27) Al-Resayes, S. I.; Hitchcock, P. B.; Nixon, J. F. *J. Organomet. Chem.* **1984**, *267*, C13.

(28) The first intermediate preceding the directly observed chelate is formulated as having one open dppm ring. This has not been directly substantiated, since we were unable to characterize it unambiguously. Nonetheless, it is a logical assignment, since ring opening must necessarily occur enroute from a bridged structure to a chelated one.

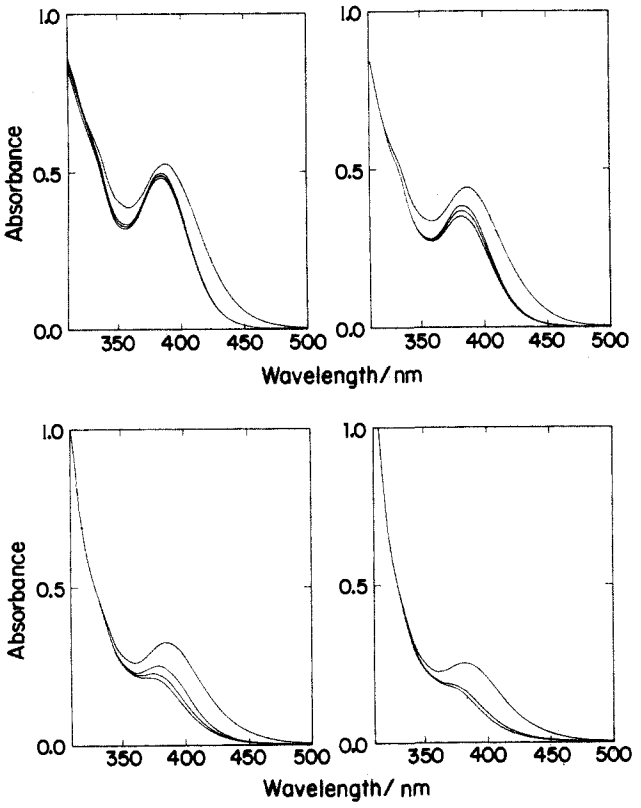

Figure 8. Showing absorbance decreases with time, as in Figure 7, taken at 5.0-min intervals, for 0.2 mM $Et_4N^+Cl^-$.

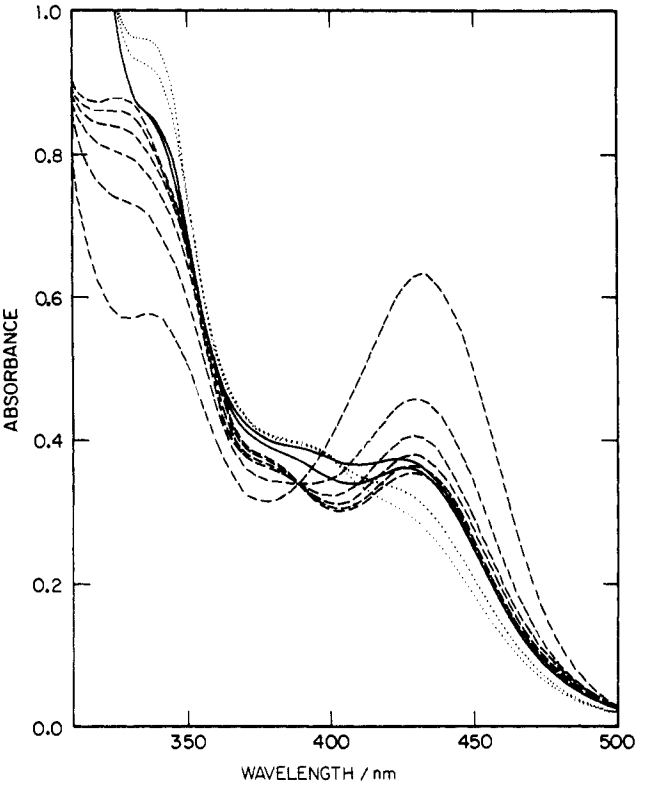

Figure 9. The reaction between $[(n\text{-butyl})_4N]I$ and $[Pt_2(\mu\text{-dppm})_2(PPh_3)_2]^{2+}$, as in Figure 7, showing the effect of adding PH_3. The dashed lines show the spectrum (decrease with time at 430 nm) at 2.0-min intervals beginning after addition of I^-. The solid lines show the effect of adding 2 mM PPh_3 12.0 min after addition of I^-; the scans were taken at 1.0-min intervals (absorbance increasing at 430 nm. The dotted lines show the spectrum 48 and 93 min after addition of the PPh_3 (absorbance decreasing at 430 nm).

that of the chelated intermediate. The well-defined isosbestic point at 388 nm indicated a transformation between only two species. With added PPh_3, however, the integrity of the isosbestic point was lost (Figure 7b), signaling the onset of $(I\text{--}PPh_3)^+$ formation. At still higher $[PPh_3]$ (Figures 7c and d), direct formation of $(I\text{--}PPh_3)^+$ became the major pathway; conversely, the chelated intermediate diminished in proportion. The rate constant for $(I\text{--}PPh_3)^+$ formation increases 60-fold over $[PPh_3] = 0$–2.0 mM. The proportion proceeding along each pathway changes owing to the growing importance of the reverse of the initial dissociation step shown in eq 10 with increasing $[PPh_3]$. The rate acceleration by added PPh_3, which is less than first order with respect to $[PPh_3]$, arises because it inhibits formation of the chelated intermediate.

When 2 mM PPh_3 is added to the iodide reaction *after* formation of the chelated intermediate, a small absorbance *increase* to followed by a very slow absorbance decrease at 428 nm. (This phenomenon is illustrated over a wider spectral region in Figure 9). The first effect arises from an increased concentration of the initial (ring-open) intermediate. Subsequent formation of $(I\text{--}PPh_3)^+$ is then limited by the rate of a chelate-opening reaction proposed in the next section, instead of the ordinary situation which would have prevailed had PPh_3 been present from the outset.

Formation of $(X\text{--}PPh_3)^+$ from the η-dppm Intermediate. This step occurs over many hours and was not studied in detail. Given the structures of the two species, the transformation clearly must entail several steps. Indeed, there is no obvious route to restore the bridging dppm *except* a second ring-open process. We thus propose, albeit on the basis of this logic and not as a direct inference from experiment, the following pathway: the η^2-dppm intermediate returns to the original ring-open form, which more slowly transforms to the final product in a multi-stage reaction. *The η^2-dppm intermediate is a dead-end intermediate as regards formation of the final product.*

Conclusions. These general patterns are evident: (1) steric factors can play a dominant role in determining the reactivity of dinuclear complexes; (2) formation of a coordinatively unsaturated platinum center is an important reaction pathway in sterically encumbered complexes; (3) changes in solvent and the addition of ionic components can greatly alter the course of the reaction.

The rates of small molecule insertion into $(Ph_3P\text{--}PPh_3)^{2+}$ are *independent* of $[PPh_3]$ (i.e., they occur by rate-limiting dissociation of the dppm–P–Pt bond); terminal ligand substitution shows the same behavior under comparable conditions. On the other hand, the latter is *retarded* by PPh_3 (under conditions where the dissociation pathway is important, i.e., with added ClO_4^- at low $[X^-]$). Thus ligand dissociation/substitution trans to the Pt–Pt bond does *not* lie along the pathway for "A"-frame formation (insertion). Considering the geometry of the "A"-frame product, that is as expected. In addition, ligand dissociation is much less important than ring-opening from the halide ion pairs ($k_{-L} \ll k_{ro}$, in the absence of ClO_4^-), despite the strong trans influence of the Pt–Pt bond.

Experimental Section

Materials. Most solvents (dichloromethane, methanol, benzene, chloroform, acetone, dichloromethane-d_2, and tetrachloroethane-d_2) were used as purchased, although for use particularly in the kinetic studies 5 parts of CH_2Cl_2 were treated with 2 parts of sulfuric acid, washed twice with 5% aqueous sodium carbonate, washed 4 times with water, and dried over $CaCl_2$. The salts $Et_4N^+Cl^-$, $(n\text{-Bu})_4N^+Br^-$, $(n\text{-Bu})_4N^+I^-$, and $(n\text{-Bu})_4N^+ClO_4^-$ were recrystallized from acetone–dichloromethane–hexanes (2:2:1), dichloromethane–diethyl ether, dichloromethane–hexanes, and ethanol, respectively. Triphenylphosphine was recrystallized either from ethanol or dichloromethane–hexanes.

The dinuclear platinum(I) complexes $[Pt_2(\mu\text{-dppm})_2Cl_2]$ and $[Pt_2(\mu\text{-dppm})_2(PPh_3)_2](PF_6)_2$ were prepared by literature methods.[7a,25] They were identified by their UV–vis and NMR (^1H and ^{31}P) spectra.[5,7a,25] The isolation and identification of the previously unknown 1:1 complexes $[Pt_2(\mu\text{-dppm})_2X(PPh_3)]PF_6$ have been described separately.[9] The iodo–chelate intermediate, $[Pt_2(\mu\text{-dppm})(\eta^2\text{-dppm})(PPh_3)]^+$, was prepared in solution in ca. 70% yield by addition of a tenfold excess of $(n\text{-Bu})_4NI$ to a 16 mM solution of $[(Ph_3P\text{--}PPh_3)^{2+}](PF_6^-)_2$ in dichloromethane. The chloro–chelate was prepared analogously, although the yield[13] did not exceed 25%. These thermally unstable intermediates showed resonances in the ^{31}P NMR spectrum which were completely absent in the reactant and product. The complexes were characterized by their UV–vis spectra

and, after stabilization at −20 °C, their ^{31}P spectra.

Methods. The $^{31}P\{^1H\}$ NMR spectra were recorded at 121.5 MHz on a Bruker WM 300 spectrometer with appropriate temperature control for spectra recorded below ambient temperature. Splitting patterns were simulated by using software (NIC-SIM) provided with the Nicolet NT-300 spectrometer. The latter instrument was also used for routine ^1H spectra. UV–vis spectra and the kinetics measurements in the slower reactions were measured on a Cary Model 219 spectrophotometer. Kinetic data were fit to suitable equations by standard least-squares programs. More rapid reactions were monitored at suitable wavelengths on a Canterbury Model SF-3A stopped-flow spectrophotometer interfaced with an OLIS 3820 Data System for data collection, storage, and analysis.

Acknowledgment. This work based in part on the Ph.D. thesis of R.J.B., was supported by the U.S. Department of Energy, Office of Basic Energy Sciences, Division of Chemical Sciences, under Contract W-7405-ENG-82. The Nicolet NT-300 NMR spectrometer was purchased in part with funds to the Department of Chemistry at Iowa State University from a Grant (No. CHE-3209709) from the National Science Foundation.

Mimics of Transaminase Enzymes

R. Breslow,* A. W. Czarnik,[1] M. Lauer,[2] R. Leppkes,[3] J. Winkler,[4] and S. Zimmerman[5]

Contribution from the Department of Chemistry, Columbia University, New York, New York 10027. *Received August 28, 1985*

Abstract: Pyridoxamine has been attached to the primary side and to the secondary side of β-cyclodextrin; the resulting compounds convert α-keto acids to amino acids with substrate selectivity and some stereoselectivity. Pyridoxamine has also been attached to a synthetic macrocycle; the attached binding group showed substrate selectivity. Chains carrying catalytic basic groups have been attached to pyridoxamine; appropriate systems catalyze the prototropic rearrangement characteristic of transamination. A catalyzed HCl elimination involving chloropyruvic acid was also observed. A tetrahydroquinoline system related to pyridoxamine was synthesized to permit the stereochemically defined placement of a basic catalytic group. This converted keto acids to amino acids with good stereoselectivity for the formation of optically active products.

Pyridoxal phosphate and pyridoxamine phosphate are the two central coenzymes of amino acid metabolism.[6] The synthesis of almost all amino acids is achieved by the biochemical reaction of pyridoxamine phosphate with α-keto acids, in one of the steps of an overall process referred to as transamination (Figure 1). The pyridoxamine phosphate is converted to pyridoxal phosphate, the other coenzyme form; this can react with a second amino acid to regenerate pyridoxamine phosphate and convert the amino acid to its corresponding keto acid. As a result, a keto acid and an unrelated amino acid interchange functionality. Of the order of 30 different transaminase enzymes have been identified, which are reasonably specific for the particular pair of amino acid/keto acid reactants whose functionality is catalytically interchanged.

Pyridoxal phosphate has a number of other functions as well. Indeed it is the coenzyme for most of the interesting metabolic transformations of amino acids, catalyzing such processes as α-decarboxylation, β-decarboxylation, α,β-elimination reactions, β-substitution reactions (as in the reaction of serine with indole to form tryptophan), etc. In all of these cases the first step is the formation of a Schiff base between the pyridoxal phosphate aldehyde group and the amino group of the amino acid. The subsequent detailed chemistry is determined by the specific conformation of this adduct and of enzymatic catalytic groups within the enzyme–substrate–coenzyme complex.

The pioneering work of Snell[7] and of Braunstein[8] helped to clarify the mechanisms of all these reactions. It was shown that in simple model systems pyridoxal (with or without its phosphate group) and pyridoxamine could perform essentially all of the reactions in which they are involved metabolically. The rates in these nonenzymatic reactions were very slow, and the characteristic selectivities of the enzymatic processes were not present.

Considerable improvement in rate could be achieved in these model systems when polyvalent metal cations were included,[9] although no evidence has been found for the requirement of any such cations in enzymatic reactions. Metal complexing in the model system helps to fix the geometry of the coenzyme–substrate Schiff base, a task performed by the enzyme in the biochemical reaction. Martell showed[10] that there are situations in which nonaqueous solvents (that may better mimic the interior of the enzyme) can have an advantage in pyridoxal model reactions.

Some years ago we started a series of studies on model systems for these transaminase enzymes, with several goals. First of all, we wanted to incorporate more of the features of the enzymatic system itself. In particular, we wanted to incorporate a binding group to increase the extent of capture of the substrate and add some selectivity to the processes. In transaminase enzymes the protein itself helps to bind particular substrates, in cooperation with the covalent binding to the coenzyme. Furthermore, the enzyme acts to catalyze the steps of the transamination process.

(1) NIH postdoctoral fellow, 1981–1983. Current address: Department of Chemistry, The Ohio State University, Columbus, OH.
(2) Holder of the Liebig Postdoctoral Fellowship of the Fonds der Chemischen Industrie. Current address: BASF AG, Hauptlaboratorium, Ludwigshafen/Rh., W. Germany.
(3) NATO postdoctoral fellow, 1982–1983. Current address: BASF AG, Kunststofflaboratorium, Ludwigshafen/Rh., W. Germany.
(4) American Cancer Society postdoctoral fellow, 1981–1983. Current address: Department of Chemistry, University of Chicago, Chicago, IL 60637.
(5) Taken in part from: Zimmerman, S. Ph.D. Thesis Columbia University, 1983. Current address: Department of Chemistry, the University of Illinois, Urbana, IL 61801.
(6) For reviews, see: Bruice, T. C.; Benkovic, S. "Bioorganic Mechanisms"; W. A. Benjamin: New York, 1966; Vol. 2, Chapter 8. Walsh, C. "Enzymatic Reaction Mechanisms"; W. H. Freeman: San Francisco, CA 1979; Chapter 24. Note that in enzymatic transaminations the lysine Schiff base of pyridoxal phosphate is the catalytically important structure, rather than the free aldehyde.
(7) Ct.: Metzler, D. E.; Ikawa, M.; Snell, E. E. *J. Am. Chem. Soc.* **1954**, *76*, 648–652 and earlier papers.
(8) Braunstein, A. E.; Shemyakin, M. M. *Biohimiya (Moscow)* **1953**, *18*, 393.
(9) Metzler, D. E.; Snell, E. E. *J. Am. Chem. Soc.* **1952**, *74*, 979–983.
(10) Martell, A. E.; Matsushima, Y. "Pyridoxal Catalysis: Enzymes and Model Systems"; Interscience: New York, 1963; pp 32–52. Martell, A. E.; Matsushima, Y. *J. Am. Chem. Soc.* **1967**, *89*, 1331–1335.

0002-7863/86/1508-1969$01.50/0